EFFECT OF METASTABLE ATOMS IN RF ARGON DISCHARGES

by

Marisa Roberto

Memorandum No. UCB/ERL M00/23

19 May 2000

EFFECT OF METASTABLE ATOMS IN RF ARGON DISCHARGES

by

Marisa Roberto

Memorandum No. UCB/ERL M00/23

19 May 2000

ELECTRONICS RESEARCH LABORATORY

College of Engineering
University of California, Berkeley
94720

Prof. Marisa Roberto was a Visiting Scholar from Brazil with the Plasma Theory and Simulation Group in the EECS Department from late February 1999 until late May 2000. She most graciously volunteered to develop two additions to the Monte Carlo Collision (MCC) part of our PIC-MCC many-particle plasma codes. We are very grateful for these additions, which will be widely useful and are already incorporated into our plasma device codes.

Prof. Charles K. (Ned) Birdsall, for the Plasma Theory and Simulation Group.

EFFECT OF METASTABLE ATOMS IN RF ARGON-DISCHARGES

Marisa Roberto

Department of Electrical Engineering and Computer Sciences,

University of California, Berkeley, California, 94720

Visiting Scholar, EECS, Berkeley, CA. Period: Mar/99 - May/00

Permanent address: ITA/CTA, S. Jose dos Campos, Sao Paulo, 12228, Brazil - e-mail: marisar@fis.ita.cta.br

Abstract

A planar one-dimensional particle-in-cell simulation with Monte Carlo Collisions (XPDP1) has been used to study 13.56 Mhz argon discharge including metastable species. Reactions such as metastable creation, ionization from the metastable state, metastable quenching to resonant level and metastable-metastable collision were taken into account. It was found that the metastable density profile has a peak near the plasma/sheath interface at a pressure of 1 Torr, due to the high production rate of metastables near this interface. Quenching to resonant level and step wise ionization are not dominant reactions to loss of metastables. A comparasion between discharges with and without metastables is presented. The effect of pressure and applied voltage is also verified.

1. Introdution

The lowest four excited states of argon atom, designated at $1s_5$, $1s_4$, $1s_3$ and $1s_2$, include two metastable levels $1s_3$ and $1s_5$, which cannot decay to any lower levels via optically allowed transitions. They have lifetimes of $>$ 1.3 s and 3.8 s, respectively[1]. Once formed, the metastable densities are often significant compared to those ground-state atoms, due to their very long lifetimes. Furthermore, the cross section for the metastable states are two or three orders of magnitude greater than those of the ground state. In low temperature plasmas, it is important to include metastable states due to the combination of large cross sections and low threshold energies.

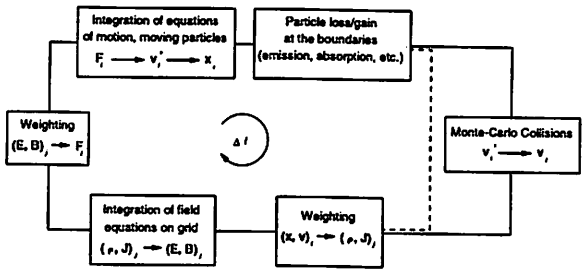

Figure 1: The flow chart for an explicit PIC scheme with the addition of the Monte Carlo condition package, called PIC-MCC.

In the present work, the planar one-dimensional particle in cell simulation with Monte Carlo Collision package is used to study a 13.56 MHz rf argon discharge including metastable species. Fig. 1 shows the flow chart for a PIC-MCC scheme. The effect of pressure and applied voltage is verified. A comparison between discharges with and without metastables also is presented.

2. Collision Types

The reactions considered in the argon model are:

(1) $e + Ar \longrightarrow e + Ar$ (elastic scattering)

(2) $e + Ar \longrightarrow e + Ar^*$ (excitation E=11.83eV)

(3) $e + Ar \longrightarrow e + Ar^m$ (metastable excitation E=11.55eV)

(4) $e + Ar \longrightarrow 2e + Ar^+$ (ionization E=15.76 eV)

(5) $e + Ar^m \longrightarrow 2e + Ar^+$ (ionization of metastable E=4.21eV)

(6) $Ar^m + Ar^m \longrightarrow Ar^+ + Ar + e$ (metastable pooling)

(7) $Ar^m + e \longrightarrow Ar^r + e$ (quenching to resonant)

(8) $Ar^+ + Ar \longrightarrow Ar + Ar^+$ (charge exchange)

(9) $Ar^+ + Ar \longrightarrow Ar^+ + Ar$ (elastic scattering)

The threshold energies for excitation, metastable excitation and ionization of metastables are 11.83 eV, 11.55 eV and 4.21 eV, which corresponds to transitions $1s_2$ and $1s_5$ for excitation and metastable excitation. The cross sections for these

reactions are in references (2) and (3). Metastable-metastable collisions are an energy gain process for electrons, which in this case corresponds to 7.34 eV. This is the energy output which is carried away by the electron. The cross section is very large in this case, $1.3\text{x}10^{-13} cm^{2}$[4]. This can be a important process in maintaining high electron energies in glow discharges. The $(3p^5 4p)$ states of argon lie approximately 13 eV above the ground state, but only 1.5 eV higher than $(3p^5 4s)$ states. When the argon is initially in a metastable state, excitation of the $(3p^5 4p)$ can occur because the transition requires only about 1.5 eV. A metastable in the $1s_3$ level can make a quenching collision to the resonant $3p^5 4p(2p_4)$ level. The cross section is in ref. (1) for electrons energies in the range 0-12 eV. It is small for 2-3 eV but increases quickly for energies above 4 eV ($\sigma \simeq 18\text{x}10^{-16} cm^2$). Another cross section for metastable quenching to a resonant level was taken into account, which corresponds to transitions between the level $3p^5 4s$, particularly, $1s_3 \longrightarrow 1s_2$. The cross section is very large for 12 eV ($\sigma \simeq 100\text{x}10^{-16} cm^2$), but decreases very quickly at 13 eV. For 15 eV the cross section is $\sigma \simeq 1\text{x}10^{-16} cm^2$.

It is assumed that the argon gas density (the neutral species) remains constant and uniform in space. Therefore the neutral particles are not followed as particles. In this model, the metastable excited atoms are followed as particles, allowing them to make collisions. The algoritm for determining collisons between charged and neutral species used the same method described by Birdsall[6] and Vahedi and Surendra[7].

3. Results and Discussion

The simulations modelled rf capacitive discharge with external circuit elements R=L=0 and C = 1 F. Electrode spacing L = 5 cm, electrode area A = 0.002 m^2, initial conditions for electron, ion and metastable densities were $n_e = n_i = 1.0x10^{16} m^{-3}$ and $n_{Ar}{}^m = 1.0\text{x}10^{14} m^{-3}$. The simulations were run for 300 rf cycles, until to reach the equilibrium for electrons and ions, which corresponds to time around $2\text{x}10^{-5}$ s. In order to verify pressure, voltage and metastable effects were studied the cases showed in the Table 1. The case (7) was run without metastables in order to determine their effect on the discharge properties.

with metastables			*w/o metastables*	
cases	pressure(Torr)	voltage(V)	pressure(Torr)	voltage(V)
1	1	50	-	-
2	1	200	-	-
3	1	500	-	-
4	0.05	50	-	-
5	0.05	200	-	-
6	0.05	500	-	-
7	-	-	1	500
8	1	500	-	-

Table 1. Summary of simulation results. In the case 8 quenching to resonant level and step-wise ionization were not considered.

Figure 2 shows the electron energy distribution function (eedf) at the bulk plasma for cases (1), (3), (5) and (7). The average electron temperature is 0.45, 0.57 and 0.73 eV for p = 1 Torr (cases 1, 3 and 7) and 0.60 eV for p = 0.05 Torr (case 5). As voltage increases there is not significant difference in the eedf at low electron energy. However for the low pressure case there are more electrons in the tail at higher voltages producing a slightly concave eedf. Vahedi, V. et al [9] studied an rf 2.56 A/cm^2 current driven argon discharge without metastables species and obtained an eedf which is convex at high pressures and concave at low pressures. There is no almost difference in the eedf with and without metastables for high electrons energy.

Figure 3 shows electrons, ions and metastable densities for case (5). One can see that plasma density has a peak in the middle of the discharge. In Figure 4 is shown the densities for low pressure (cases 4 and 6) in order to verify the voltage effects. For case (4) the profiles are rather flat while for case (6) the profiles has a peak in the center of the discharge. As voltage increases one has more metastables production. For case (1) the electron, ion and metastable profiles are rather flat in the bulk, as shown in Figure 5. However, at higher voltages, the metastable profile have a peak near the plasma sheath interface, as showed in Figures 6 and 7, for cases (2) and (3). The peaks are due to enchanced production of metastables due to higher energy electrons in the sheath region. Peaks in the electron density can also be seen

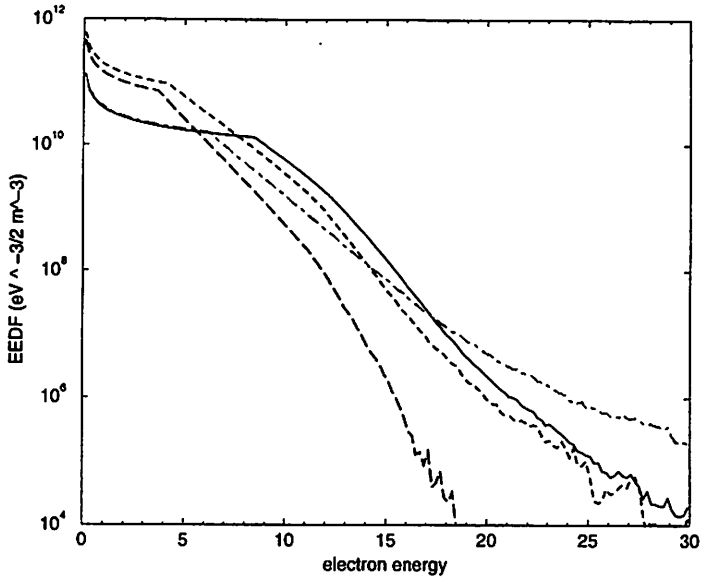

Figure 2: Electron distribution function for case (1) (long-dashed line), case (3)(dashed line), case (7) (solid line) and for case (5) (dot dashed line). Note that the knees were not identified.

which increase with increasing voltage. As the pressure increases, the sheath width decreases. The peaks in the electron density near the plasma sheath boundaries are believed to be primarily due to ionization caused by stochastic heating of the fast electrons in the driven sheaths. On the other hand, electron heating in the bulk plasma is believed to be primarily due to ohmic heating of slow electrons there, as shown in Fig. 8 for cases (2), (3), (5) and (6). For high pressure the ohmic heating is larger than stochastic heating, resulting in a peak profile for densities. Effects of stochastic electron heating was studied by V. Vahedi et al. [10].

Figure 9 shows electron and ion average densities for cases (3) and (7). High electrons energy population are lost by ionization collision with metastables. However, the rate of ionization from the metastable level is low compared with ionization rate of the ground state, i.e., Ioniz. rate from ground state/ Ionization rate from metastable $\simeq$ 5.0, considering peak values for these rates. The Ioniz. rate from ground state without metastables/with metastables $\simeq$ 1.5. It leads to a peak profile for the plasma density in the case without metastables. The average electron temperature is a little higher, Te = 0.73 eV for case (7) and 0.57 eV for the case with metastable (case 3).

Figure 10 shows ionization rate profile from ground state for case (3), which peaks near the plasma sheath interface, where the electron energy is higher. This local

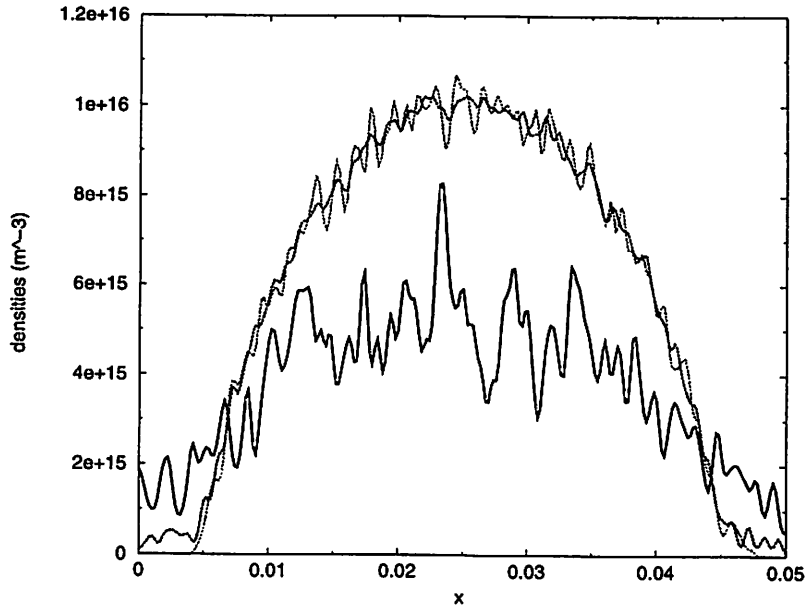

Figure 3: Electron, Ion and Metastable densities for case (5). For low pressure and V = 200 V, the profiles have a peak in the center.

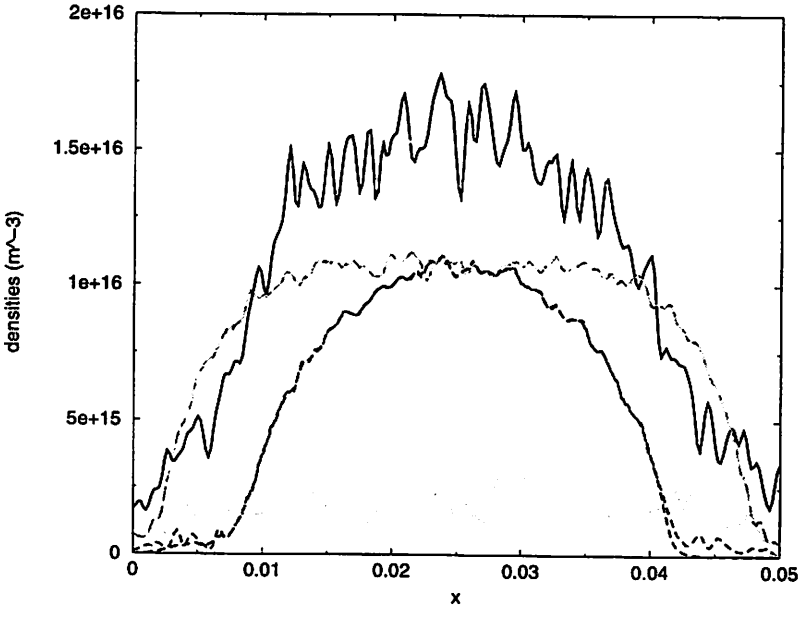

Figure 4: Electron, Ion and Metastable densities for cases (4) and (6). For low presure and low voltage, case (4), the profiles are rather flat, and have a peak in the center for high voltage, case (6).

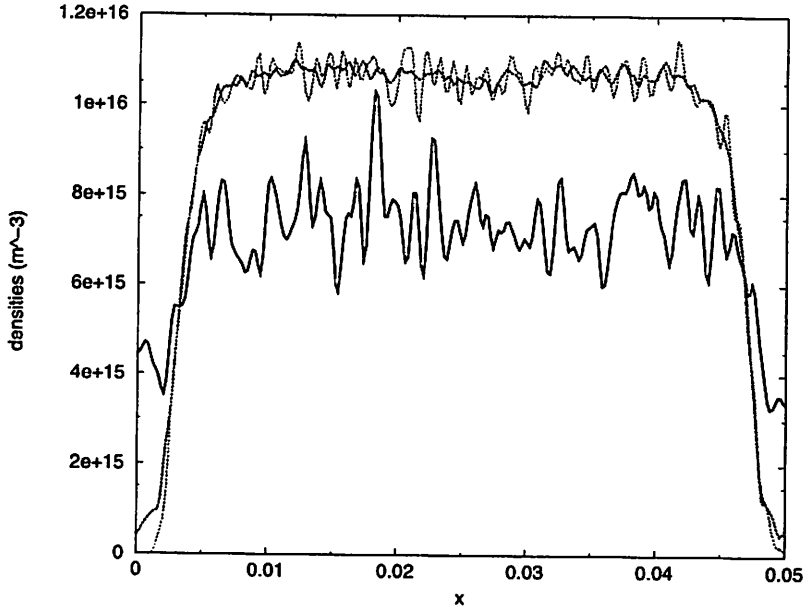

Figure 5: Electron, Ion and Metastable densities for case (1). For low voltage (V = 50 V) and high pressure (p=1 Torr) the profiles are rather flat.

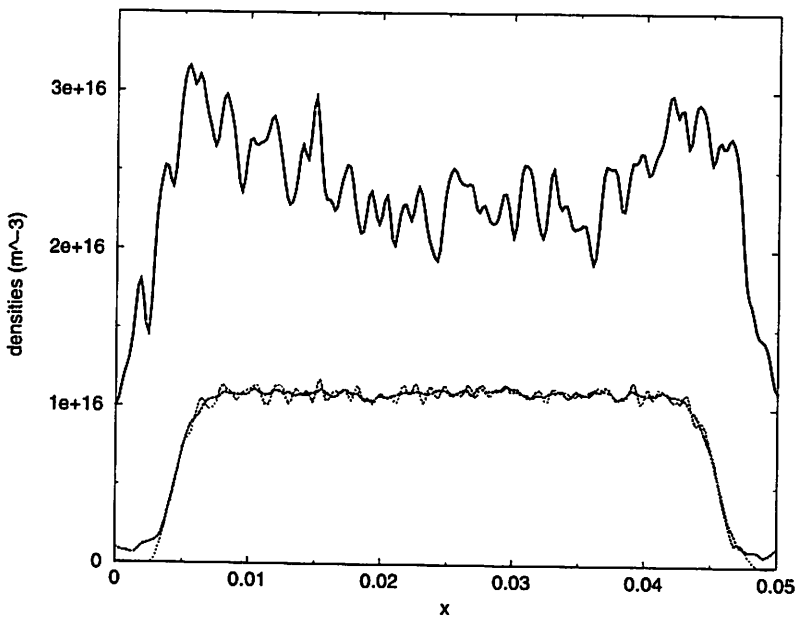

Figure 6: Electron, Ion and Metastable densities for case (2). As voltage increases for high pressure the metastable profile has a peak near the plasma sheath interface.

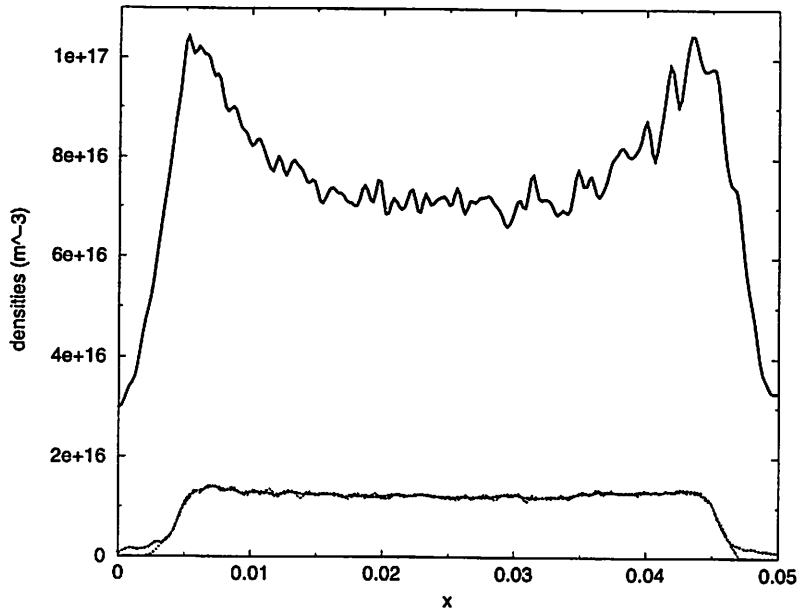

Figure 7: Electron, Ion and Metastable densities for case (3). In this case the metastable density is higher compared to the case (2).

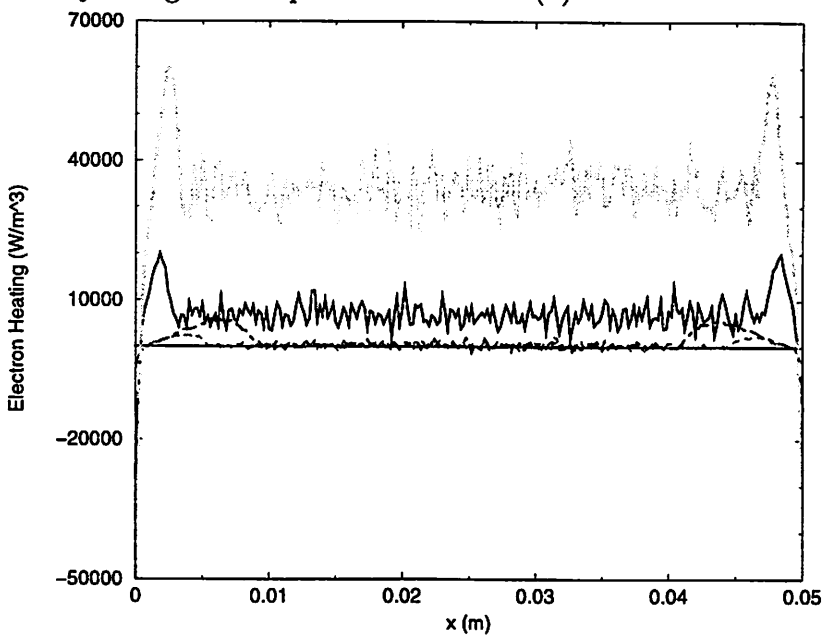

Figure 8: Electron heating rate for cases (2), (3), (5) and (6). Low pressure corresponds to dotted (V=500 V) and dashed (V=200 V) lines and high pressure corresponds to solid (V=200 V) and long-dashed line (V = 500 V).

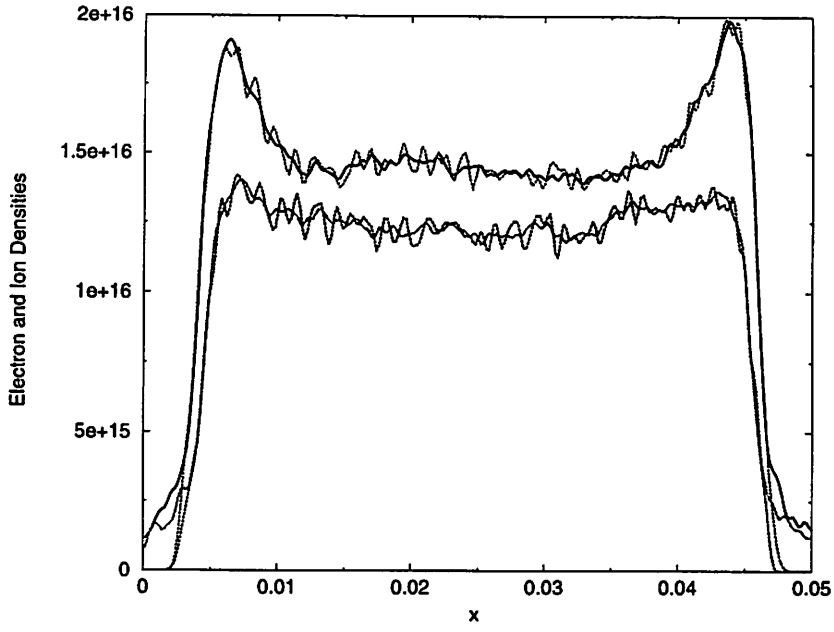

Figure 9: Electron and ion density for cases (3) and (7) with and without metastables. One can see a larger peak near the plasma sheath interface in the case without metastables.

ionization is due to stochastic electron heating produced by the oscillating sheaths and occurs when the mean free path for ionization by electrons is smaller than the discharge length. This local ionization has been observed in rf cylindrical discharge, using PDC1 code [11]. Figure 11 shows this rate for the case without metastables (case 7). The ionization rate is higher in this case.

Metastable quenching to the resonant level (reaction 7) occurs only for transition between $3p^5 4s$ ($1s_3$) to $3p^5 4p$ ($2p_4$) levels. If the cross section between $3p^5 4s$ levels is considered reaction 7 never occurs. The quenching rate is low compared to metastable creation, i.e., creation metastable ratio/loss metastable by quenching $\simeq 5.0$.

Figure 12 shows electrons, ions and metastables densities for case (8) not considering step-wise ionization and quenching to resonant. There is no very little differences in the profiles obtained in the previous case, indicating that for these conditions these reactions are not dominant to metastables loss.

Lymberopoulos and Economou [12] used a fluid simulation to study an argon rf discharge including the effect of metastables. They use the conditions f = 13.56 MHz, p = 1 Torr for pressure, L = 2.54 cm and a peak rf voltage of 200 V. They concluded

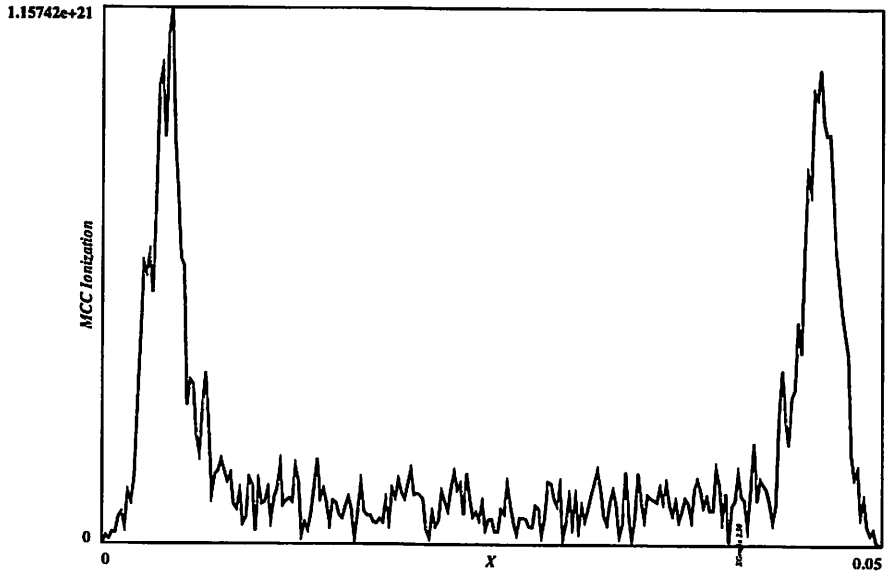

Figure 10: Ionization rate profile from ground state for case (3).

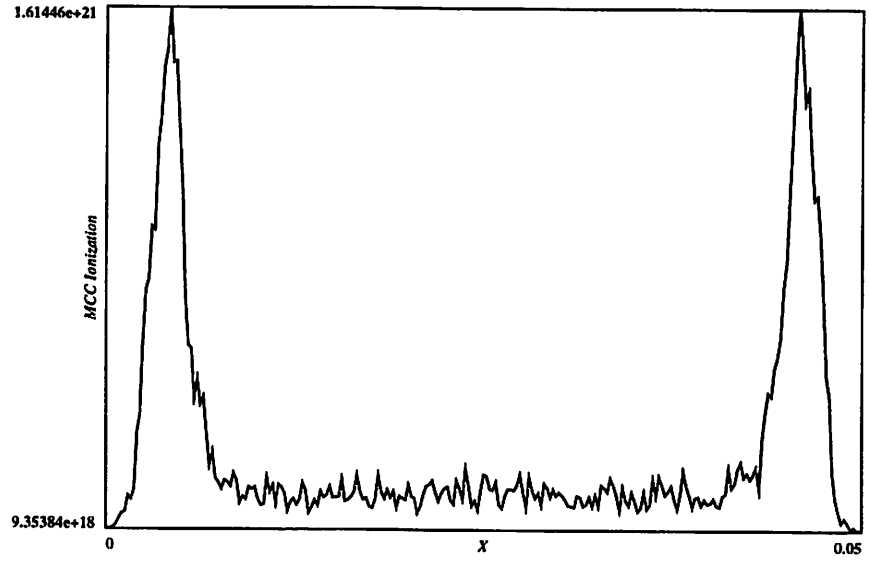

Figure 11: Ionization rate profile from ground state for case (7), which corresponds the case without metastable.

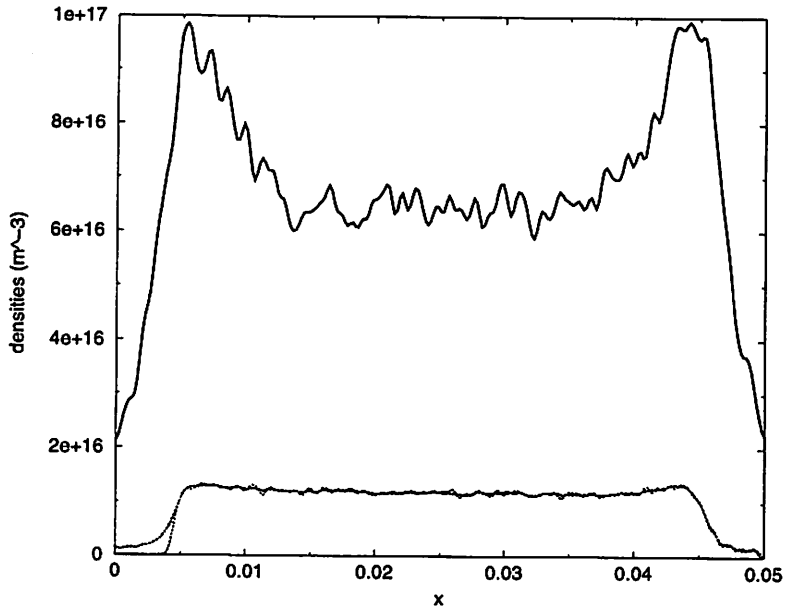

Figure 12: Electron, ion and metastable densities for pressure 1 Torr, V = 500 V. Quenching and step-wise ionization were not considered.

that electron density has a peak in the central part of the discharge and metastable density has peaks near the plasma sheath interface very similar to the profiles obtained for the PIC code. These peaks are due to enchanced production of metastables near the plasma sheath due to higher electron energy and enhanced losses of metastables by electron quenching in the central region of the discharge due to higher electron density there. For metastable quenching to resonant rate coefficient were considered transitions between $3p^5 4s$ levels. They found that electron quenching to the resonant state is the dominant loss process of metastables. Diffusion, step-wise ionization and metastable pooling follow in order of importance. They concluded metastables must be included in a rf discharge to obtain a correct description of the discharge. In order to compare this model with PIC model is showed in Fig. 13 density profiles for p=1 Torr, V=200 V and L=2.54 cm. For this condition the profiles are different that obtained using L=5 cm. There is no peak for the densities. Fig 14 shows electron heating rate for their parameters. This discharge are smaller and with a larger sheath due to the electron heating. The ohmic heating is comparable to stochastic heating. Fig 14 can be compared with Fig. 8 for case (2), where the sheath is smaller. The ohmic heating is larger to stochastic heating for a larger discharge.

However, it seems that step-wise ionization it is not dominant process for loss

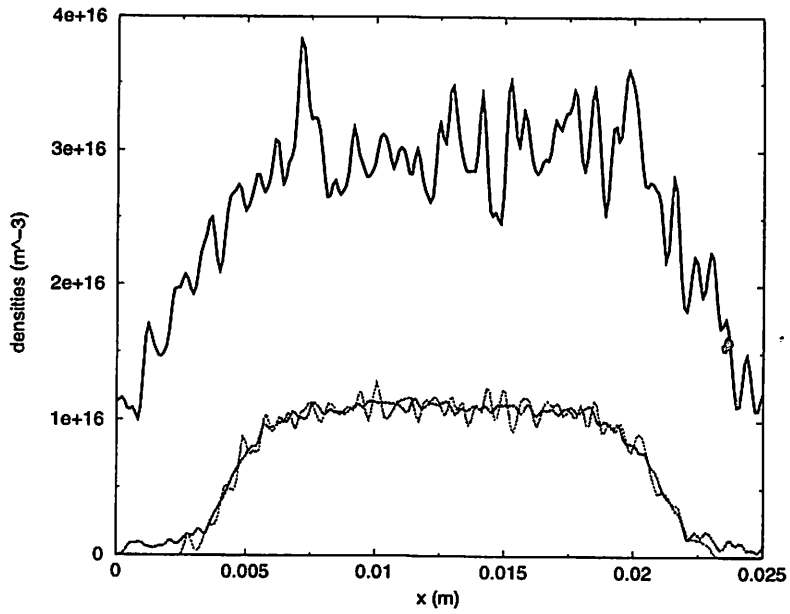

Figure 13: Density profiles for p=1 Torr, V=200 V and L=2.54 cm, which corresponds to L. and E. parameters.

argon metastables in rf discharges, due to the low rate ionization from metastable state. Besides, quenching to resonant depends on the cross section to occur and it is not a dominant process as well.

4. Conclusion

One-dimensional planar simulation with PIC/MCC model has been used to study the effect of metastable in an argon rf discharge. It has been found that metastable quenching to ressonant and metastable ionization are not the main processes of loss of metastable. The metastable profile depends on the lenght of the discharge. For 1 Torr and L=5 cm one can see a profile for metastable density which has peaks near the plasma/sheath interface and electron/ion profiles which have peaks in the same position for a given discharge lenght.

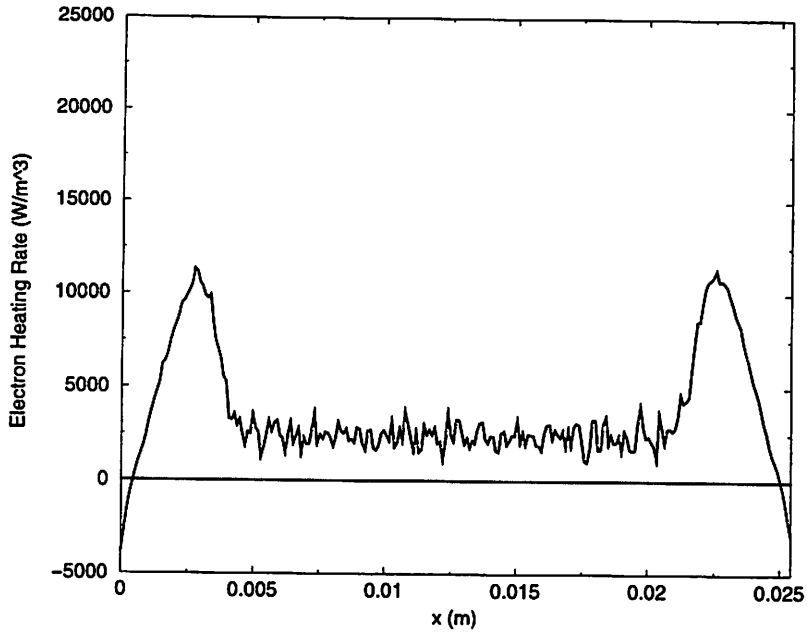

Figure 14: Electron heating rate for p=1 Torr, V=200 V and L=2.54 cm (L. and E. parameters).

5. Acknowledgments

This work has been supported by grants of the Brazilian Agency FAPESP - S. Paulo. I am grateful to Prof. C.K. Birdsall for many suggestions and reading of this work and for his kind hospitality during my Feb/1999 - May/2000 visit at PTSG group, where this work was accomplished. I am indebted to Dr. Helen Smith for many valuable comments and discussions that I believe have helped to improve this work. I also thanks the kind hospitality of the PTSG group.

6. Appendix

To access the new input files which include metastable level for argon and mixtures with argon+oxygen and argon+mercury.

- Parameter GAS in pdp1.h (pdp1h.nomixtures):

  GAS=1: Helium

  GAS=2: Argon

  GAS=3: Neon

  GAS=4: Oxygen

  GAS=5: Mercury

  GAS=8: MCC

- Parameter GAS in pdp1.h (pdp1h.withmixtures):

  GAS=1: Helium

  GAS=3: Neon

  GAS=5: Mercury

  GAS=6: Argmerc (argon+mercury)

  GAS=7: Argoxy (argon+oxygen)

  GAS=8: MCC

Note that there are two files for pdp1.h, i.e., pdp1h.withmixtures and pdp1h.nomixtures.

Replace pdp1h.* by pdp1.h to compile.

There are new makefiles for argon and mixtures. For argon:

  makefile.linux runs without metastables.

  makefile2.linux runs with metastables using a Table for cross sections

  argonm2.tbl which includes quenching to resonant level

  $1s_3 \longrightarrow 2p_4$ ($3p^5 4p$).

  makefile3.linux uses a Table for cross sections argonm.tbl which includes

  quenching to resonant level $3p^5 4s(1s_3) \longrightarrow 1s_2$.

  makefile4.linux: no quenching is considered.

  makefile6.linux: no ionization from metastable is considered.

  makefile7.linux: no quenching and ionization from metastable are considered.

For mixtures:

  makefile5.linux (It uses startmx.c and mccdiaginitmx.c)

Replace makefile*.linux by makefile to compile.

News input file parameters:

  - For mixtures one have two new parameters for pressure:

  Gpressure (for argon) and Gpressurep (for another gas).

The cross sections are in the Tables:

  - argonm2.tbl

  - argonm.tbl

  - aro2.tbl (for mixture argon+oxygen)

  - merc.tbl (for mixture argon+mercury).

References

(1) Boffard, J.B., Piech, G.A., Gehrke, M.F., Anderson, L.W., Lin, C.C. Phys. Rev. A, vol 59 (4), 2749, 1999.

(2) Madison, D.H., Maloney, C.M., Wang, J.B., J. Phys. B.; At. Mol. Opt. Phys. vol. 31, 873, 1998.

(3) Margreiter, D.; Deutsch, H., Mark, T.D. Contr. Plasma Physics 30, 4, 487, 1990.

(4) Okada, T., Sugawara, M., Japonese J. of Apl. Physics, Part. 1 vol. 35 (8), 4535, 1996.

(5) Bartschat, K., Zeman, V., Phys. Rev. A, vol. 59 (4), 2552, 1999.

(6) Birdsall, C.K., IEEE Trans. of Plasma Science, vol. 19 (2), 65, 1991.

(7) Vahedi, V., Surendra, M., Comp. Phys. Com. 87, 179, 1995.

(8) Lymberopoulos, D.P., Economou, D.J., J. Appl. Phys. 73 (8), 3668, 1993.

(9) Vahedi, V., Birdsall, C.K., Lieberman, M.A., DiPeso, G., Rognlien, T.D. Plasma Sources, Sci. Technol. 2, 273, 1993.

(10) Vahedi, V., DiPeso, G., Birdsall, C.K., Lieberman, M.A., Rognlien, T.D. Plasma Sources Sci. Technol. 2, 261, 1993.

(11) Alves, M.V., Lieberman, M.A., Vahedi, V., Birdsall, C.K. J. Appl. Phys. 69 (7), 3823, 1991.

(12) Lymberoupoulous, D.P., Economou, D.J. J. Aplly. Phys. 73 (8), 3668, 1993.